A Fuzzy Logic Classification Scheme for Selecting and Blending Satellite Ocean Color Algorithms

Timothy S. Moore, Janet W. Campbell, and Hui Feng

***Abstract*—An approach for selecting and blending bio-optical algorithms is demonstrated using an ocean color satellite image of the northwest Atlantic shelf. This approach is based on a fuzzy logic classification scheme applied to the satellite-derived water-leaving radiance data, and it is used to select and blend class-specific algorithms. Local *in situ* bio-optical data were used to characterize optically-distinct water classes *a priori* and to parameterize algorithms for each class. Although the algorithms can be of any type (empirical or analytical), this demonstration involves class-specific semi-analytic algorithms, which are the inverse of a radiance model. The semi-analytic algorithms retrieve three variables related to the concentrations of optically active constituents. When applied to a satellite image, the fuzzy logic approach involves three steps. First, a membership function is computed for each pixel and each class. This membership function expresses the likelihood that the measured radiance belongs to a class with a known reflectance distribution. Thus, for each pixel, class memberships are assigned to the predetermined classes on the basis of the derived membership functions. Second, three variables are retrieved from each of the class-specific algorithms for which the pixel has membership. Third, the class memberships are used to weight the class-specific retrievals to obtain a final blended retrieval for each pixel. This approach allows for graded transitions between water types, and blends separately tuned algorithms for different water masses without suffering from the "patchwork quilt" effect associated with hard-classification schemes.**

***Index Terms*—Algorithms, fuzzy logic, remote sensing.**

I. Introduction

In OCEAN color remote sensing, bio-optical algorithms are employed to derive information about constituents affecting the upwelling spectral radiance. The water-leaving radiance, measured in visible and near-infrared bands, contains information about the concentrations of chlorophyll a, colored dissolved organic matter (CDOM), and suspended sediments. Algorithms used in the past with the coastal zone color scanner (CZCS) and currently with the sea-viewing wide field-of-view sensor (SeaWiFS) are statistical or empirical in origin, and are primarily used to derive phytoplankton pigment or chlorophyll concentration as an index of biomass. Although these algorithms are applied globally, it is recognized that they are strictly applicable only to case 1 waters where the optical properties are governed by phytoplankton and covarying decay products [1].

Manuscript received February 7, 2000; revised August 28, 2000. This work was supported in part by NASA Contract NAS5-96063, MODIS Instrument Team Investigation and NASA Grant NSG5-6289, Office of Earth Science, Oceanography Program.

The authors are with the Ocean Process Analysis Laboratory, University of New Hampshire, Durham, NH 03824 USA (e-mail: tim@rheya.sr.unh.edu).

Publisher Item Identifier S 0196-2892(01)05478-X.

It is widely accepted that a universal bio-optical algorithm applicable for all water types is not feasible. In ocean color image scenes, there are often multiple water types with differing optical properties, which in turn require different algorithms. The most obvious example is the presence of so-called case 2 waters in coastal areas. Case 1 algorithms simply fail or return inaccurate retrievals in case 2 waters. Among case 2 waters, however, there are many different substances found globally that affect the optical properties of the water. A single parameterized case 2 algorithm should be able to account for variability in the concentrations of two or three substances, but not variability due to the wide variety of substances found globally. Thus, we are often presented with different case 2 algorithms derived for local waters, or for specific situations such as CDOM-dominated or sediment-dominated waters. While there has been a lot of effort devoted to developing case 2 algorithms [2]–[7], scant effort has been applied to address the problem of merging algorithms for different water types. A unifying scheme is needed that will not only choose which algorithm is best for a given satellite pixel but will blend retrievals from different algorithms in a manner that is physically meaningful.

The decision as to which algorithm to apply may be viewed as a classification problem. The application of a hard classification scheme that selects only one algorithm and rules out the others will often result in a "patchwork quilt" effect. This effect can be seen in retrieval images as discontinuities between water types, or it might also be manifested in ways that are not readily visible in the images but observable in other formats. The latter situation occurred in the standard processing of CZCS images where the algorithm switched between two different radiance-ratio algorithms. This produced discontinuities that were not obvious in the images, but clearly seen in discontinuous, bimodal chlorophyll histograms. In transition zones where pixels could belong to case 1 or case 2, one might have very different chlorophyll retrievals depending on which algorithm is applied. As a consequence, use of a hard classifier would result in uneven or discontinuous retrievals.

Ocean waters with different biogeochemical composition often have different optical properties. These different waters can be identified by their spectral reflectance characteristics. Remote sensing reflectance is defined as

$$R_{rs} = \frac{L_u(0^-)}{E_d(0^-)} \tag{1}$$

where $L_u(0^-)$ is the upwelling radiance and $E_d(0^-)$ the downwelling irradiance just below the air–water interface.

Semi-analytical algorithms are based on relatively simple models that relate the remote sensing reflectance to the inherent optical properties of the water, which in turn are modeled as functions of constituent concentrations. The optical properties of these substances (e.g., phytoplankton pigments, colored dissolved organic matter, organic detritus, and sediment) vary among water types, making it difficult to parameterize a single model to accommodate such variability. An alternative approach would be to parameterize models for each water type and devise a scheme for selecting the appropriate model.

In this paper, we introduce the concept and application of fuzzy logic to ocean color satellite images. Fuzzy set theory can be used not only to classify ocean pixels but also to effectively blend different algorithms together. A fuzzy classification method allows for pixels to be assigned partial or graded class memberships to different water types with which they share spectral characteristics. This is accomplished by using a fuzzy membership function that expresses the likelihood that a pixel, with its observed radiance vector, belongs to a class with a known reflectance distribution. Given a number of plausible classes, the class memberships can then be used to weight the output of class-specific algorithms. The overall effect is that transitions between water types in the output image or scene are smooth and gradual.

Fuzzy classification of satellite imagery has been used in land remote sensing for over a decade to allow for mixed land classes within a pixel [8], [9], and more recently with advanced very-high resolution radiometer (AVHRR) imagery [10]. In this latter case, ice pixels in polar images from the AVHRR were classified using fuzzy logic to allow for pixels with part sea-ice and part cloud-free ocean. While these same concepts can be applied to ocean color images to accommodate pixels that are mixtures of different water types, in a broader sense, their use reflects the ambiguity present in differentiating water types.

A. Fuzzy Logic

Fuzzy set theory allows an element to have membership to one or more sets, whereas classical set theory specifies that set membership is exclusive. Zadeh [11] first introduced fuzzy set theory as a mathematical way to represent vagueness that naturally exists in imprecise information. It extends the concepts of classical set theory and allows for partial or intermediate set membership values. It also can allow for full ("crisp" or "hard") memberships and thus is a superset of classical set theory.

In mathematical terms, let $\mathbf{S}$ denote a universe of discourse that contains elements given by $\boldsymbol{x}$ ($\mathbf{S} = \{\boldsymbol{x}\}$). In classical set theory, given a subset $\mathbf{A}$ of $\mathbf{S}$, each element $\boldsymbol{x}$ either belongs to $\mathbf{A}$ or does not belong. Membership in $\mathbf{A}$ is defined by the function

$$f_A = \begin{cases} 1, & (\text{if } x \in A) \\ 0, & (\text{if } x \notin A) \end{cases} \tag{2}$$

where f_A is called the membership function.

Under fuzzy set theory, the membership function is altered to allow for graded memberships and is transformed into

$$0 \leq f_i(\boldsymbol{x}) \leq 1 \tag{3}$$

to express partial set membership to the ith set. For *constrained* fuzzy sets [12]

$$\sum_{i=1}^{c} f_i(\boldsymbol{x}) = 1. \tag{4}$$

In this sense, $f_i(\boldsymbol{x})$ represents the probability that $\boldsymbol{x}$ belongs to the ith set, and the c sets are all possible sets. Equation (4) is not always required, however, and when this restriction is lifted, we have the case of an unconstrained fuzzy set. Either case may be "hardened" to obtain a crisp membership, and $\boldsymbol{x}$ is then assigned membership to a single class. In the case of unconstrained fuzzy sets, $f_i(\boldsymbol{x})$ might still represent the likelihood of membership to set i. Such would be the case, for example, if the likelihood of belonging to a given set is determined strictly from the properties of that set, without considering properties of the other sets. There may be high likelihood of belonging to more than one set based on incomplete or ambiguous information, in which case, the sum of f_is could exceed 1. In other situations, the c sets may not represent all possible sets and thus, a given observation might have low probability of belonging to any of the c sets. In such a situation, the sum of f_is would fall short of 1. The application of fuzzy logic to the satellite ocean color data will be unconstrained, as shown later.

Ocean Color Satellite Application: These concepts can be applied to ocean color satellite imagery where the sets or "classes" are optically distinct waters, and the elements are image pixels. It is first necessary to establish how we define an ocean water class and second to define a membership function that will assign pixels membership to these water classes.

Since Morel and Prieur [1], the accepted view of the ocean is that of a two-class system, with a majority of the ocean belonging to case 1 and a much smaller amount to case 2. This view is simple and works well as a conceptual model. However, it is not adequate as a basis for classifying remote sensing observations that are based on radiance or reflectance alone. Case 1 and case 2 waters are defined by the type of suspended particles or dissolved material in the water acting on the light field and therefore, information about the water constituents is required for classification purposes. In fact, the distinction between case 1 and case 2 waters does not rely on the measured light field at all. Since ocean color satellite sensors detect the emergent radiant light field from the ocean, it is natural (and in fact necessary) to base classification on this information.

In order to classify an image pixel based on its spectral reflectance, the spectral reflectance characteristics of the distinct water sets or classes must be defined. These sets or classes and their reflectance characteristics can be defined by performing a cluster analysis on a data base of *in situ* measurements of remote sensing reflectance. The data base ideally should include a complete representation of all possible water types. The statistical properties (multivariate probability density function) for each class or cluster found in the data base then becomes the basis for defining membership to each class. A class membership function [satisfying equation (3)] can be defined to express the likelihood of observing the measured reflectance given that the pixel belongs to a class with a known reflectance distribution. A membership function $f_i(\boldsymbol{x})$ is computed for pixel $\boldsymbol{x}$ to

each class i ($i = 1, 2, \ldots c$), and these values are used to weight the retrievals from class-specific algorithms.

The class-specific algorithms can be defined independently. They might be empirical algorithms such as radiance-ratio algorithms (e.g., [13]) or be semi-analytic in nature (e.g., [14]). In this paper, we utilize a set of semi-analytic algorithms that have been parameterized for each water class. Semi-analytic algorithms are based on analytical models that relate the reflectance or radiance, which are apparent optical properties (AOPs) to the inherent optical properties (IOPs), specifically, the absorption and backscattering coefficients [15]. The IOPs are then related empirically to the constituent concentrations. The algorithm parameterization requires a concurrent data set of concentrations, AOPs, and IOPs, and involves the fitting of "submodels" relating the IOPs to the measured constituents (e.g., a model relating the phytoplankton absorption coefficient to the chlorophyll a concentration). Conceptually, the different classes may be thought of as waters having different substances affecting their optical properties. Each parameterized submodel is designed to relate the IOP to variations in the concentration of the particular material, but a different submodel is needed when the mix of substances changes.

Final constituent retrievals for each pixel are then determined by weighting each of the class-specific retrievals in proportion to its class membership function. In practice, only those classes with membership values above a certain threshold are plausible and hence, retrievals need not be obtained for classes that are implausible.

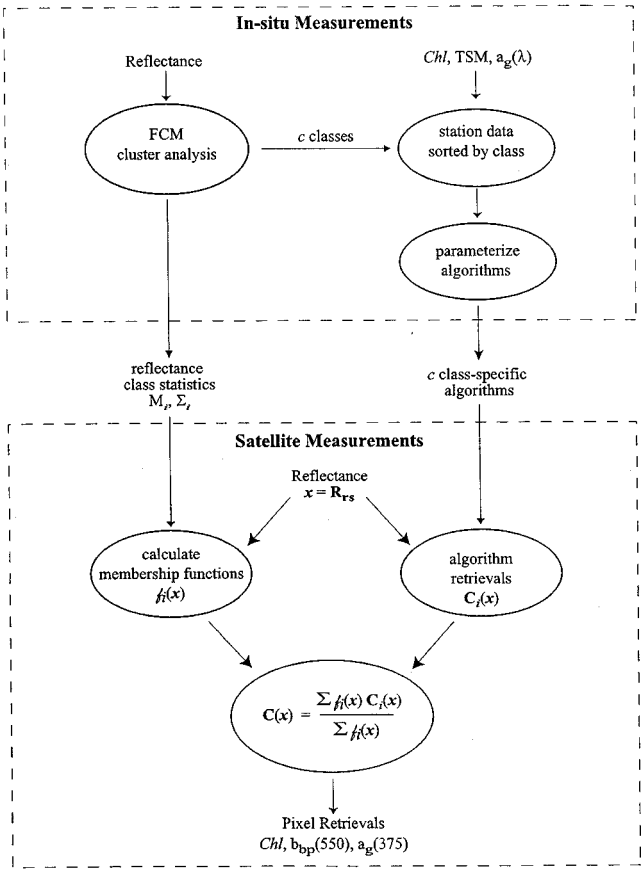

Fig. 1. Flowchart of the complete fuzzy scheme for blended algorithm retrievals. The upper dashed box depicts the methods applied to *in situ* measurements to identify classes and develop class-specific algorithms. The lower dashed box charts the application of the fuzzy scheme to satellite data.

II. Methods

The overall strategy (Fig. 1) begins with the development of a data base for parameterizing bio-optical algorithms, and for defining and characterizing optically distinct water classes. We have chosen the northwest Atlantic continental shelf as our study area and have assembled a data set of *in situ* bio-optical measurements made in the Gulf of Maine, Middle Atlantic Bight, and Sargasso Sea by various investigators (Table I). We were also interested in testing whether or not a data set from outside the study region was applicable to this region, and so a data set from Tokyo Bay [16] was included. This amounted to a total of 159 stations from which AOP, IOP, and constituent concentration data were pooled.

To combine all the data from the various cruises, IOP and AOP data had to be transformed into similar units. For the AOP data, all but the Tokyo Bay data were based on the remote sensing reflectance R_{rs}. Tokyo Bay data were irradiance reflectance ($R = E_u/E_d$) measurements that we converted to R_{rs} with the following equation:

$$R_{rs} = \frac{R}{Q} \tag{5}$$

where Q is the ratio of upward irradiance to upward radiance. Although this factor is known to vary from 3 to 5 sr^{-1} for typical satellite viewing angles [17], we used a constant value of 4.5 sr^{-1} for the purposes of this study.

For the coastal mixing and optics (CMO) cruises (Table I), bulk water-column absorption coefficients were computed using optically-weighted averages [18] of the ac-9 (WET Labs, Inc.) profile data, with optical weights derived from the diffuse attenuation coefficient as determined from the AOP profiles. IOP data for the Coastal Services Center (CSC) and Tokyo Bay data sets were obtained from surface bottle samples. In all cruises,

TABLE I

SUMMARY OF *IN SITU* DATA USED FOR THIS ANALYSIS. THE DATA SOURCES WERE: NOAAs COASTAL SERVICES CENTER (CSC), DATA PROVIDED BY A. SUBRAMANIAM; COASTAL MIXING AND OPTICS (CMO) EXPERIMENT, DATA PROVIDED BY A. BARNARD OF OREGON STATE UNIVERSITY, CORVALLIS, H. SOSIK, WOODS HOLE OCEANOGRAPHIC INSTITUTE, WOODS HOLE, MA, AND C. ROESLER, BIGELOW LABORATORY FOR OCEAN SCIENCES, WEST BOOTHBAY HARBOR, ME. BERMUDA BIO-OPTICAL PROGRAM (BBOP) AND TOKYO BAY DATA BOTH OBTAINED FROM THE SEABASS ARCHIVE AT NASA GSFC, GREENBELT, MD. THE BBOP DATA WERE CONTRIBUTED BY D. SIEGEL AND N. NELSON, AND THE TOKYO BAY DATA WERE CONTRIBUTED BY M. KISHINO

Cruise	Dates	Location	# Stations	Constituents
CSC May96	5/96	Gulf of Maine	25	*Chl, TSM*
CSC Jun97	6/97	Gulf of Maine	12	*Chl, TSM*
CMO96	8/96 - 9/96	MAB Shelf	31	*Chl*
CMO97	4/97 - 5/97	MAB Shelf	12	*Chl*
BBOP	1/95 - 12/96	Bermuda	34	*Chl*
Tokyo Bay	2/82 - 6/84	Tokyo Bay	45	*Chl, TSM*

surface chlorophyll measurements were made, but surface measurements of total suspended matter (TSM) were available for the CSC and Tokyo Bay cruises only. No IOP measurements were available for the BBOP data at the time of this analysis.

A. Cluster Analysis—Step One

An unsupervised clustering based on the fuzzy c-means (FCM) cluster algorithm [19] was applied to the *in situ* R_{rs} data (here the bold font indicates a vector, comprised of the $\mathbf{R}_{rs}$ data at six wavelengths (412, 443, 490, 510, 555 and 670 nm) corresponding to the first six bands of SeaWiFS). We employed the FCM algorithm available in MATLAB, Math Works, Inc. This algorithm produces a fuzzy clustering of the data into a specified number of clusters. The algorithm is based on minimizing an objective function J_m defined as

$$J_m = \sum_{k=1}^{c} \sum_{i=1}^{N} (u_{ik})^m |\boldsymbol{x}_i - \nu_k|^2 \tag{6}$$

where

u_{ik}	membership of the ith observation to the kth cluster;
$\lvert\boldsymbol{x}_i - \nu_k\rvert$	Euclidean norm between vectors $\boldsymbol{x}_i$ and ν_k;
m	weighting exponent that can be any real number greater than 1 (typically set to 2);
c	number of clusters;
N	number of observations.

The basic function of this algorithm is to choose clusters that minimize the distance between the data points and the prototype cluster centers (represented by the vectors ν_k). Cluster centers are iteratively adjusted until optimization criteria are met (e.g., maximum number of iterations or minimum change residual). The membership function used in MATLAB is attributed to Bezdek [19] and is based on the reciprocal of the distance between points, whereas our subsequent application of the fuzzy classification to satellite imagery used a different membership function as described later.

The number of clusters to be returned by the FCM clustering algorithm is determined *a priori* by the input parameter c. We clustered the data several times, varying both c and the weighting exponent m and used two measures of cluster validity to determine the optimal number of clusters. The first measure was the partition coefficient F [19], [20]. This validity function ranges from 0 to 1 and measures the amount of overlap between clusters. A partition coefficient of one indicates no cluster overlap or no membership sharing between clusters, while a low F value indicates overlap between clusters and weak clustering. Thus, a high partition coefficient is desired. Although this is a good indicator of cluster separation, the function only considers membership values and ignores the structure of the data.

We also used a second validity function, the compactness and separation index S, which involves membership values and data structure [21]. The S cluster validity function is a fraction in which the numerator is a measure of the variance within clusters, and the denominator is the minimum distance between cluster centers. The goal is therefore to obtain a small S indicating a clustering where the clusters are compact and separate from each other.

TABLE II
SUMMARY OF RESULTS FOR CLUSTER VALIDITY FUNCTIONS F (PARTITION COEFFICIENT) AND S (COMPACTNESS AND SEPARATION INDEX)

	m									
c	1.2		1.5		2		2.5		3	
	F	S	F	S	F	S	F	S	F	S
3	0.96	0.43	0.83	0.24	0.69	0.39	0.59	0.31	0.52	0.22
4	0.94	0.45	0.87	0.31	0.72	0.26	0.59	0.18	0.49	0.11
5	0.96	0.25	0.89	0.22	0.74	0.16	0.56	0.10	0.43	0.07
6	0.97	0.20	0.90	0.17	0.67	0.18	0.50	0.29	0.38	0.15
7	0.96	0.42	0.87	0.44	0.64	0.39	0.46	0.19	0.34	0.11
8	0.96	0.43	0.85	0.24	0.62	0.27	0.41	0.50	0.30	0.16

Clusters were generated for a range of initial conditions (c ranging from three to eight and m ranging from 1.2 to 3.0) in an attempt to objectively determine the optimal number of clusters for the data set of 159 remote sensing reflectance values. The results of the two cluster validity functions F and S over the range of initial conditions are shown in Table II. These results suggested that there were six clusters and the best choice for m was either 1.2 or 1.5. In actuality, the assignment of the 159 data points to the six clusters did not change for the two values of m.

Once the classes (clusters) were identified, the mean reflectance spectrum $\mathbf{M}_i$ and covariance matrix Σ_i were calculated for each class. Other station data (e.g., Chl, TSM, etc.) were sorted into their respective classes and then used to parameterize class-specific algorithms (see step two) (note: the Bermuda BBOP data comprised two classes, and since IOP data were not available for Bermuda at the time of the analysis, we used the model of Garver and Siegel [14], which was parameterized for Bermuda.)

B. Algorithm Parameterization—Step Two

The semi-analytic algorithms were based on bio-optical models of the remote sensing reflectance that were parameterized with *in situ* data for each class. All models were based on the relationship between $\mathbf{R}_{rs}$ and IOPs given by

$$\boldsymbol{R}_{rs} = \sum_{i=1}^{2} l_i \left(\frac{b_b}{a + b_b} \right)^i \tag{7}$$

where $l_1 = 0.0949$, and $l_2 = 0.0794$ [22]. The absorption coefficient was modeled with three subcomponents

$$a = a_w + a_p + a_g \tag{8}$$

where a_w, a_p, and a_g are the absorption coefficients for seawater, particulates, and colored-dissolved material. The backscattering coefficient b_b was

$$b_b = b_{bw} + b_{bp} \tag{9}$$

where b_{bw} is the seawater backscattering coefficient, and b_{bp} is the particle backscattering coefficient. The a_w and b_{bw} values are assumed to be known constants and were taken from Pope *et al.* [23].

Using the *in situ* data from each class, relationships were derived between the IOP terms in (8) and (9) and three variables to be retrieved by the algorithms: the chlorophyll concentration, Chl; the absorption of colored dissolved organic matter and detritus at 375 nm, $a_g(375)$, which is a measure of the concentration of these organic decay products; and particle backscattering $b_{bp}(550)$, which is a measure of the total suspended matter concentration. Each water class had unique submodel parameters derived from the *in situ* data for that class, and the structure of the various IOP submodels was not uniform across the water classes. Here we omit details of the algorithms because our purpose is to demonstrate the application of the fuzzy classification scheme. Substantially more data would be necessary to develop robust algorithms and assess their accuracy.

C. Fuzzy Classification—Step Three

The satellite data were converted from normalized water-leaving radiance $\mathbf{L}_{wN}$ to in-water remote sensing reflectance $\mathbf{R}_{rs}$ as follows (spectral subscripts suppressed):

$$R_{rs} = \frac{L_{wN}}{F_0 M + rQL_{wN}} \tag{10}$$

where

F_0	extraterrestrial solar irradiance;
$Q(=4.5)$	ratio of upwelling irradiance to upwelling radiance [see (5)];
$M(=0.53)$	term that accounts for the effects of reflection and refraction at the air–water interface;
$r(=0.48)$	water–air reflectance for totally diffuse upward irradiance.

The original expression in [22] defined $\mathbf{L}_{wN}$ as a function of $\mathbf{R}_{rs}$, whereas (10) is an inversion of that equation to obtain $\mathbf{R}_{rs}$. For more details, see [22].

The class membership function for the measured reflectance spectrum $\mathbf{R}_{rs}$ was then defined as follows. A measure of the separation between $\mathbf{R}_{rs}$ and the ith class mean $\mathbf{M}_i$, is the squared Mahalanobis distance

$$Z_i^2 = (\mathbf{R}_{rs} - \mathbf{M}_i)^t \Sigma_i^{-1} (\mathbf{R}_{rs} - \mathbf{M}_i) \tag{11}$$

where Σ_i is the covariance matrix of the ith class, and t indicates the transpose of the vector $(\mathbf{R}_{rs} - \mathbf{M}_i)$. The Mahalanobis distance [24] is the multivariate equivalent of the standardized random variable $Z = (X - M)/S$, which is the distance of the univariate random variable X from its mean M normalized by the standard deviation S. In this study, a common covariance matrix, the average of all the class covariance matrices, was substituted in place of Σ_i for all class membership computations (see Section IV).

If the distribution of $\mathbf{R}_{rs}$ vectors belonging to class i is multivariate normal, and $\mathbf{R}_{rs}$ belongs to class i, then Z^2 has a χ^2 distribution with n degrees of freedom (where n is the dimension of $\mathbf{R}_{rs}$). As a measure of likelihood that $\mathbf{R}_{rs}$ is drawn from class i, we define the membership function to be

$$f_i = 1 - F_n(Z_i^2) \tag{12}$$

where $F_n(Z^2)$ is the cumulative χ^2 distribution function with n degrees of freedom. The $F_n(Z^2)$ function was evaluated using IDL routines (Research Systems, Inc., Boulder, CO), which approximated the function as a finite series. These class membership values satisfy (3), but do not sum to 1, and thus the fuzzy sets are unconstrained.

D. Algorithm Inversion—Step Four

A Gauss–Newton nonlinear optimization method was used to invert the remote sensing reflectance models to retrieve Chl, $a_g(375)$ and $b_{bp}(550)$ [14]. This inversion scheme requires an initial guess, which is then iteratively adjusted until a minimum residual error was satisfied between the observed and modeled $\mathbf{R}_{rs}$ spectra. The initial guess for Chl was obtained from the OC4 chlorophyll algorithm which is the standard algorithm used by the SeaWiFS project [25], and class means were used as initial guesses for $a_g(375)$ and $b_{bp}(550)$.

The final blended retrieval for each pixel was a weighted sum of the retrievals of all class-specific algorithms that were determined as "plausible." A class was considered plausible if two criteria were met. First, the class membership had to be above a minimum threshold, which was arbitrarily set at 0.0001. This conserved processing time by screening out classes whose mean reflectance spectra were not sufficiently close to the observed spectrum. Secondly, Chl retrievals from any class-specific inversion had to be within a range of chlorophyll values determined from the class statistics. This screened for unrealistic output values from the inversion optimization. The class retrieval was weighted based on its membership function. This weight was equal to the class membership value normalized by the sum of all plausible membership values.

III. Results

A. Cluster Analysis

The FCM clustering process resulted in six optically distinct classes being identified from the *in situ* reflectance data (Fig. 2). Generally, the resultant classes were composed of stations from the same source or geographic region (Table III). For example, class 1 was mainly composed of the CMO data sets, which were from stations located just south of Georges Bank, and class 2 was mainly composed of data from the CSC May96 cruise, whose measurements were from stations in Gulf of Maine coastal areas. Likewise, classes 5 and 6 were composed of measurements from the BBOP data set and represent "blue-water" classes. All of the class 4 stations and most of the class 3 stations were from the Tokyo Bay data set. The remaining Tokyo Bay stations were assigned to classes 1 and 2, apparently sharing $\mathbf{R}_{rs}$ characteristics with CMO data and CSC May96 data.

Concentrations of TSM, Chl, and CDOM associated with classes 1 through 4 are shown in Fig. 3. In all three plots, two distinct groups appear: one comprised of classes 1 and 3 and another comprised of classes 2 and 4. Classes 1 and 3 have lower relative levels of the three constituents (Table IV) and have overlapping concentration domains as defined by the boxes in the figure. However, the class mean $\mathbf{R}_{rs}$ spectra (Fig. 4) are very different for these two classes. Although both curves show a peak at 490 nm, the overall magnitudes are very different. Class 3 has much higher reflectance values at all wavelengths com-

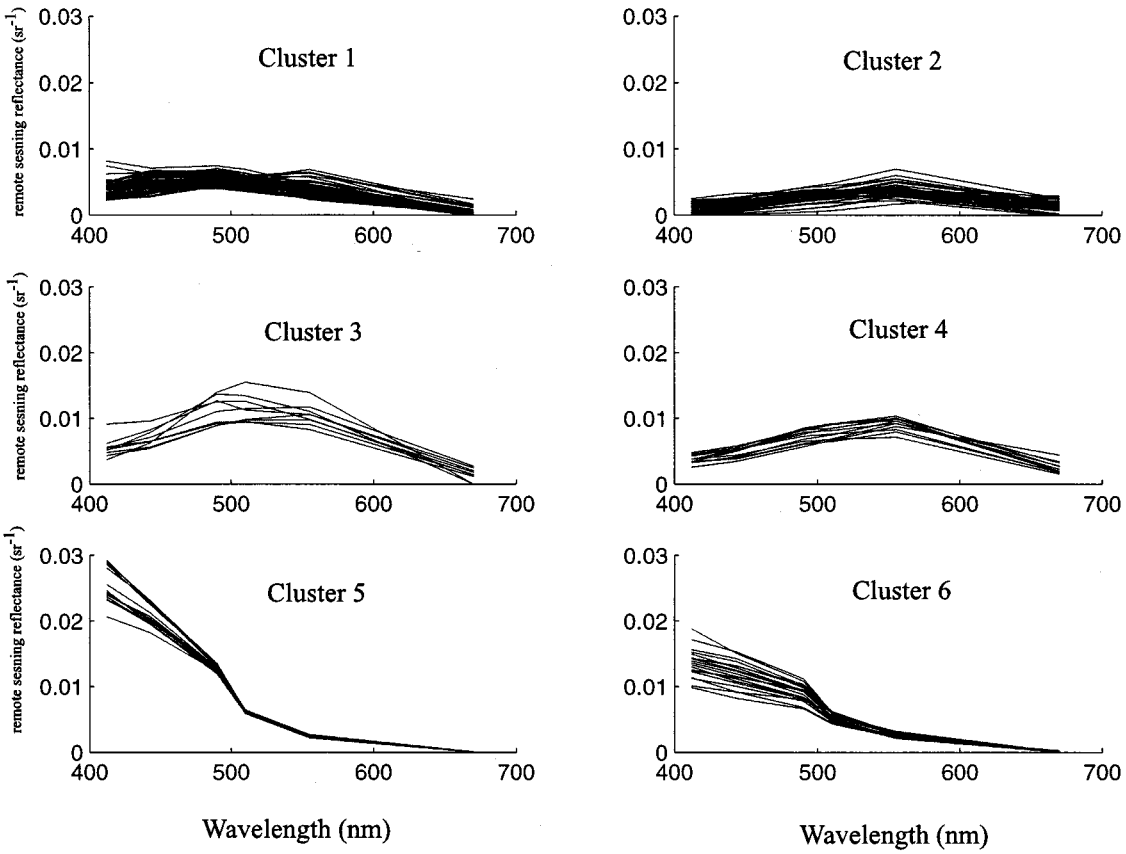

Fig. 2. Reflectance spectra associated with each class (cluster). Top left: Class 1, $N = 65$, top right: Class 2, $N = 39$, middle left: Class 3, $N = 9$, middle right: Class 4, $N = 12$, bottom left: Class 5, $N = 15$, and bottom right: Class 6, $N = 19$.

TABLE III
DISTRIBUTION OF CRUISE STATIONS AMONG THE WATER CLASSES IDENTIFIED FROM AN UNSUPERVISED CLUSTERING OF THE REMOTE SENSING REFLECTANCE DATA

Cruise	#Stations	#Station/Class					
		1	2	3	4	5	6
CSC May96	25	-	25	-	-	-	-
CSC Jun97	12	6	4	2	-	-	-
CMO96	31	30	1	-	-	-	-
CMO97	12	11	1	-	-	-	-
BBOP	34	-	-	-	-	15	19
Tokyo Bay	45	18	8	7	12	-	-

pared to class 1. Likewise, classes 2 and 4 also have overlapping concentration domains but different class mean $\mathbf{R}_{rs}$ spectra. The mean spectra for classes 2 and 4 share a peak at 555 nm, but have different magnitudes. This suggests that other factors such as particle size and composition are causing variations in the light field that distinguish one water type from another.

B. Classification Maps

The class membership maps for a SeaWiFS image taken over the northwest Atlantic on October 8, 1997 are shown in Fig. 5. Pixels with high membership ($f_i > 0.9$) are colored white, and little or no membership ($f_i < 0.1$) are black. Intermediate memberships are shades of gray. There were three dominant classes that emerge in examining these membership maps. Pixels with high membership in class 1 appear along the Middle Atlantic Bight (MAB) shelf and southern flank of Georges Bank, with some moderate to high membership in the Gulf of Maine and low membership along the north wall of the Gulf Stream. This is geographically consistent with the locations of the *in situ* stations that were clustered into class 1, which were primarily from the CMO data set located just south of Georges Bank. Likewise, pixels with high membership in class 2 were located in coastal waters in the Gulf of Maine and around the flank of Georges Bank. The stations that were clustered into this class were predominantly from the CSC May96 cruise in the Gulf of Maine (Table III, Fig. 4). Membership to this water class is diminished outside this region. The membership maps also show that class 6 is associated with the Gulf Stream but not the adjacent Sargasso Sea. Remnant Gulf Stream water in the form of a warm-core ring in the slope water is also apparent in this membership map, whereas the slope water has no membership to this class. Areas over Georges Bank and near and in the Bay of Fundy have membership in classes 3 and 4 (although this is not easily discernible in Fig. 5). These areas of high tidal energy generally exhibit high concentrations of suspended sediments. Classes 3 and 4 were formed from stations with high amounts of suspended sediments, although many of these stations were from the Tokyo Bay data set and thus were not located on Georges Bank or the Bay of Fundy.

The sum of the membership values for the six classes is shown in Fig. 6. Areas that are colored black contain pixels that do not

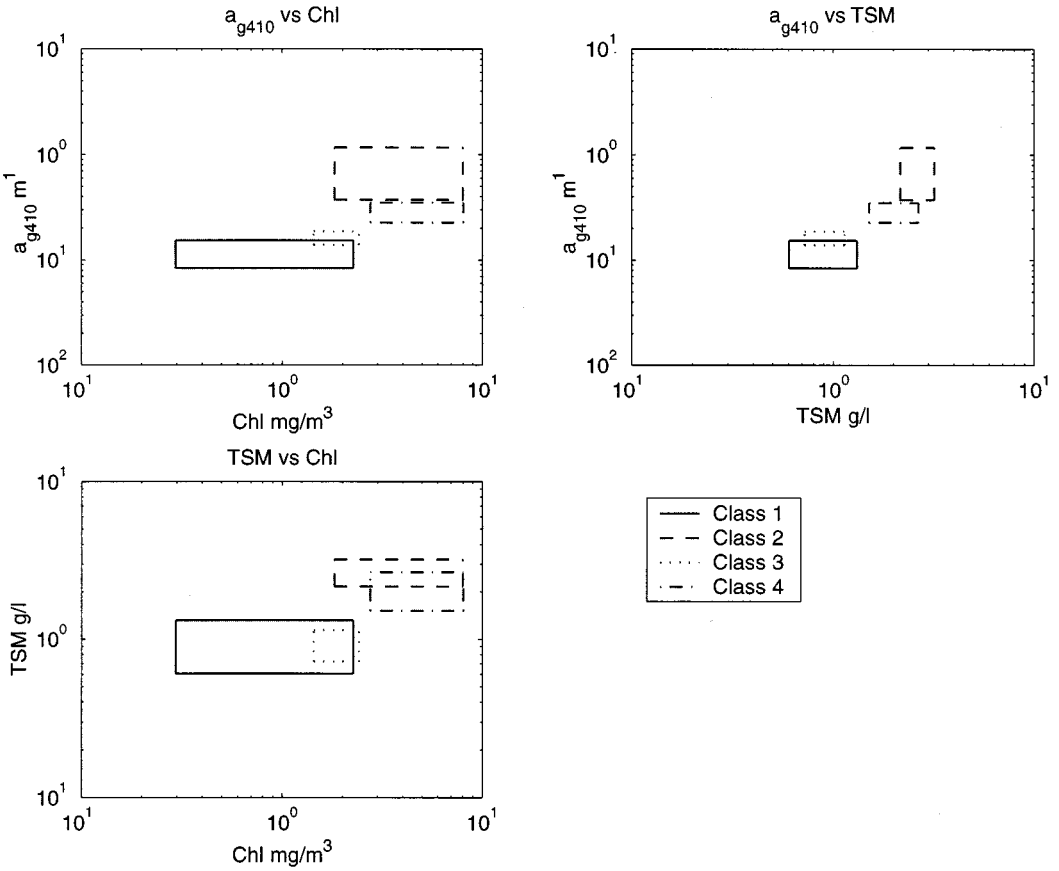

Fig. 3. *In situ* measurements grouped according to the reflectance class assignments (classes 1–4 only). (Top left) $a_g(410)$ versus Chl, (top right) $a_g(410)$ versus TSM, and (bottom left) TSM versus Chl. The boxes are formed from the mean value plus or minus 0.5 standard deviations (one standard deviation across).

TABLE IV
IN-WATER CONSTITUENT CLASS MEAN CONCENTRATIONS AND STANDARD DEVIATIONS

Constituent	Class Means					
	1	2	3	4	5	6
Chl (mg/m^3)	1.28	4.91	1.93	5.40	0.07	0.29
TSM (g/l)	0.96	2.67	0.93	2.09	-	-
a_g(410) (m^{-1})	0.12	0.77	0.16	0.29	-	-

Constituent	Class Standard Deviations					
	1	2	3	4	5	6
Chl (mg/m^3)	1.97	6.17	0.97	5.27	0.04	0.16
TSM (g/l)	0.71	1.03	0.42	1.15	-	-
a_g(410) (m^{-1})	0.07	0.80	0.05	0.14	-	-

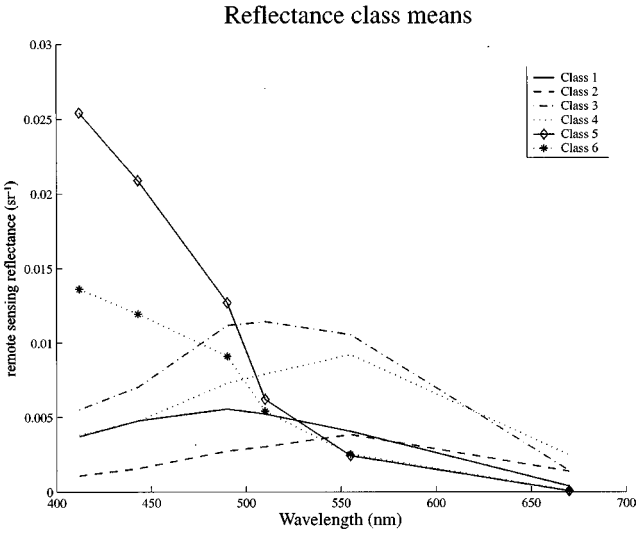

Fig. 4. Mean reflectance spectra for classes 1–6. These class curves were used in the membership function along with a common covariance matrix to assign class membership values to satellite pixel observations.

belong to any of the represented classes, and the darker gray pixels have low membership in all classes (membership sum < 0.4). These areas include portions of the Gulf of Maine, the slope waters between the MAB shelf and north wall of the Gulf Stream, and the Sargasso Sea. It is precisely these areas that are lacking representation in the *in situ* data base.

The final constituent images were weighted retrievals from algorithms for the classes that were considered "plausible." Although it is possible for all six algorithms to be applied to a given pixel, there were typically between 1 and 3 algorithm inversions per pixel (Table V). Of all the pixels in the image, roughly half (45%) were evaluated with a single class algorithm, while most of the remaining half (42%) were solved with two algorithms. Less than 0.1% required more than three algorithms, whereas a significant number (8.7%) had no plausible classes and thus no retrieved value. This situation arose in image areas with op-

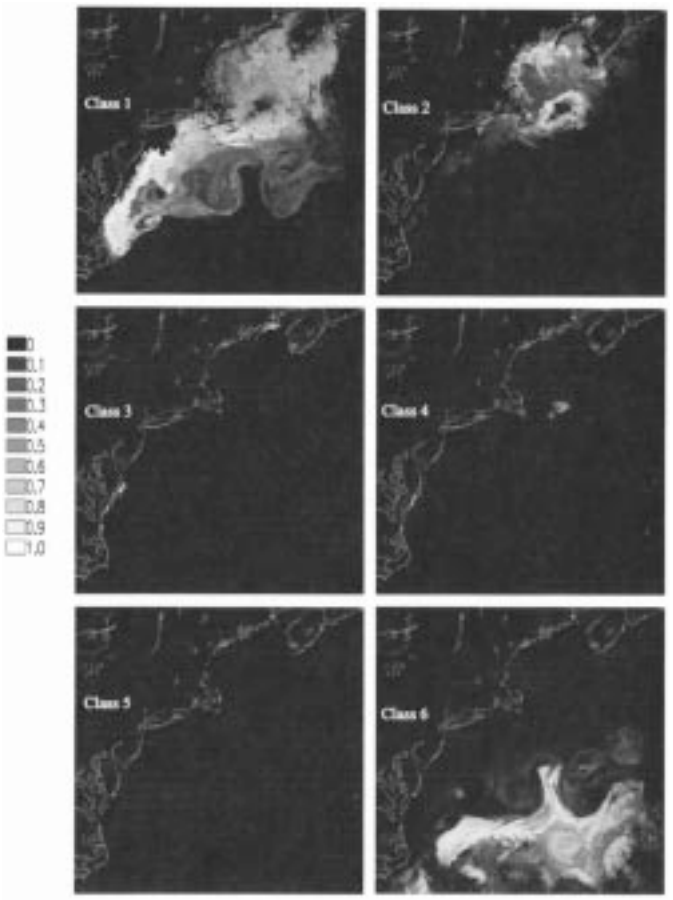

Fig. 5. Class membership maps generated for a SeaWiFS image acquired over the northwest Atlantic Ocean on October 8, 1997. Pixel membership values are related to the probability that the pixel belongs to the class indicated in each panel.

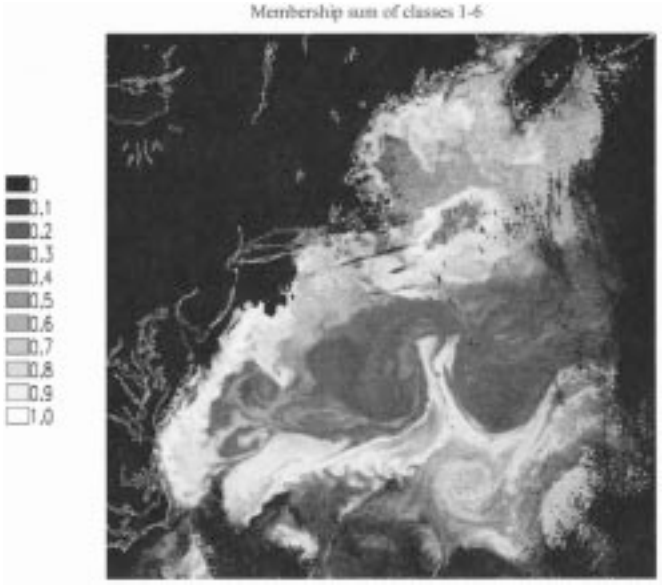

Fig. 6. Map showing the sum of class memberships calculated by totaling the six individual class membership values at each pixel.

TABLE V
NUMBER OF PLAUSIBLE CLASSES FOR PIXELS IN THE OCTOBER 8, 1997 SeaWiFS IMAGE

# plausible classes	# pixels	%
0	49,973	8.7
1	255,237	44.6
2	238,213	41.6
3	28,355	5.0
4	118	< 0.1
5	0	0
6	0	0
Total	571,896	100.0

tical properties that were poorly represented in the pool of *in situ* data. These areas include parts of the Sargasso Sea, Pamlico Sound, and some (but not all) areas within the Chesapeake Bay and the Bay of Fundy.

C. Constituent Retrieval Maps

The blended retrievals are presented in Fig. 7, along with the standard (OC4) chlorophyll derived by the SeaWiFS Project. The blended Chl image (a) compares favorably with the SeaWiFS OC4 chlorophyll values (b). Unlike Chl, there are no standard products for $a_g(375)$ or $b_{bp}(555)$ to compare to these retrievals. The range of values produced in the $a_g(375)$ image (c) is comparable to values reported in previous studies [26]–[28], and previous estimates of $b_{bp}(555)$ [14], [29] are on the order of 10^{-3} to 10^{-4} m^{-1}, which is the general range seen in the (d) image. The three retrieval images are shown here chiefly to illustrate the fact that semi-analytic algorithms involve a simultaneous solution for three covarying variables, which influence the optical properties of the water. The concentration patterns in the three retrieval images exhibit similar features and structures. This is consistent with the covarying relationships in the *in situ* data.

In general, the three blended retrieval images show smooth, continuous patterns. Scattered pixels with discontinuous values can be seen in the slope waters south of Long Island and along the MAB shelf/slope front, most notably in the Chl and $a_g(375)$ images (a) and (c). This area was not represented in our *in situ* data base and consequently, poorly represented by the algorithms. Membership values in these waters were low for all of the classes, although the minimum threshold was set low enough for these pixels to pass the membership criterion. It is our expectation that with a larger and more comprehensive *in situ* data base, these effects will vanish.

IV. DISCUSSION

A. Ocean Classification

Classification of ocean water types was introduced by Jerlov [30] and was based on the transmittance of downwelling irradiance in the surface layer. Jerlov [31] later identified 12 optically different classes of ocean water ranging from oceanic to coastal. Morel and Prieur [1] classified ocean water into two classes (case 1 and case 2) based on the type of absorbent particle suspended in the water column. Classification schemes based on other criteria have also been put forth [32]–[35]. The fuzzy logic

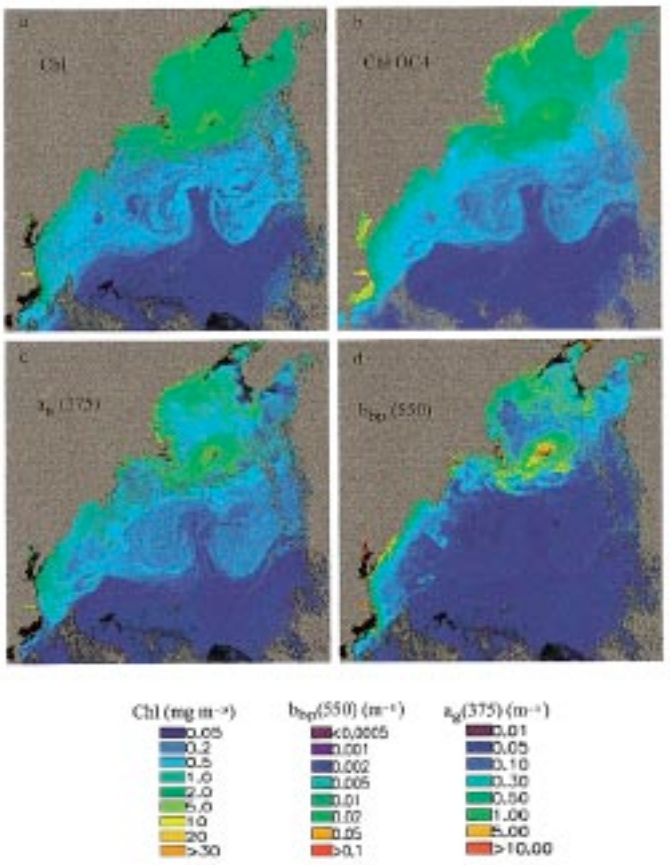

Fig. 7. Retrieval images (a) Chl, (b) standard SeaWiFS Chl image using the OC4 algorithm, (c) $a_g(375)$, and (d) $b_{bp}(550)$.

classification scheme introduced here is based on concepts utilized in land remote sensing and involves clustering *in situ* optical data into discrete classes based on measured reflectance spectra. The characterization of classes is then used as a basis to extend partial class memberships to satellite pixels and the membership function is used as a basis for blending retrievals from different class-specific algorithms.

Qualitatively, the fuzzy scheme achieved a smooth blending of the different bio-optical models tailored to the different water types without showing abrupt changes in retrieved values, except where they occur naturally in the image scene. To assess the performance of the scheme quantitatively requires a validation data set that was not available. However, we can examine other aspects of the results, such as the class membership maps, to ask whether the classification makes sense. The class membership maps that were derived are governed by the *in situ* data that were used to obtain the classes. Depending then on the *in situ* data, the classes and thus the membership maps could change. A larger, more comprehensive data set would presumably converge to give a stable characterization of the various classes.

We believe that a finite number of classes exist in the world's oceans. The six classes identified in this study may be found elsewhere. The inclusion of the Tokyo Bay data set suggests the hypothesis of global optical classes. The Tokyo Bay station data were distributed over four classes (Table III). Approximately half of the Tokyo Bay stations shared characteristics with data in our study area (classes 1 and 2), whereas the other stations (those in classes 3 and 4) were generally not characteristic of the other *in situ* data from our study area. These classes contained stations with high amounts of suspended matter, and their $\mathbf{R}_{rs}$ curves (Fig. 4) show high values from 440 to 550 nm. Although there are geographic regions in the image that are known to be turbid and contain high amounts of suspended sediments (Bay of Fundy, Chesapeake Bay, Georges Bank) and exhibit some membership to classes 3 and 4, these areas overall had low membership sums, and remain poorly classified. This suggests that the physical characteristics of suspended matter (particularly mineral sediments) play an important role in influencing the shape of $\mathbf{R}_{rs}$ curves, and sediment-dominated classes may be region-specific. This also underscores the high degree of variability in case 2 waters.

Assuming the classes that were found in the *in situ* data have optical properties that remain stable over time, the classification maps can provide useful information regarding feature tracking. In this regard, if the optical properties of any measurable ocean phenomenon are known (e.g., coccolithophore blooms), they can be used as the basis of a "class" that can then be tracked in ocean color images.

B. Interpretation of Fuzzy Memberships

In terrestrial remote sensing applications that use a fuzzy classification methodology, partial membership values represent pixels with mixed compositions or coverage types. The reflectance spectra for macroscopic mixtures, where individual components occur as homogeneous patches, have been shown to be linear combinations of endmembers in the mixture [36]. Endmembers in this sense are coverage types that cannot be further subdivided into smaller types (e.g., as forests, fields, rocky soils). Membership values for macroscopic mixtures truly are the proportion of endmembers present contributing to the reflectance signal.

Fuzzy memberships do not have the same meaning for a reflectance signal that is affected by a microscopic or "intimate" mixture, where the components are randomly distributed within the field of view (FOV) of the instrument [36]. This situation is analogous to that of mineral reflectance spectroscopy. It has been shown that for microscopic mixtures of minerals, the reflectance signal is a nonlinear combination of reflectance spectra of the endmembers present [37]. The problem becomes linear to a first order for microscopic mixtures when considering the single scattering albedo [38]. That is, the total single scattering albedo can be represented as a linear combination of endmember albedos.

The ocean reflectance spectrum can also be viewed as the result of a microscopic mixture of substances and indeed, the need to account for different substances in the water is the basis for using different class-specific bio-optical models. In these models, the effects of the microscopic elements on the reflectance is clearly nonlinear. Thus, the linear mixing of two or more model results (retrievals) via the fuzzy scheme proposed here is inappropriate mathematically from the perspective of a microscopic mixture. However, the linear weighted sum of retrievals is not intended to represent a true mixture of waters within the pixel. Instead, our use of the weighted retrieval is

rooted in a statistical or Bayesian argument. It reflects the inherent ambiguity associated with incomplete information.

Consider the goal of estimating a property $\mathbf{C}$ given the observation $\mathbf{R}$. It is established that there are c distinct classes $\{\mathbf{R}\}_i$ within the universe of $\mathbf{R}$ values such that the relationship between $\mathbf{C}$ and $\mathbf{R}$ depends on the class to which $\mathbf{R}$ belongs. Thus, the best estimate ("expected value") of $\mathbf{C}$ given $\mathbf{R}$ is

$$E(\mathbf{C}|\mathbf{R}) = \sum_{i=1}^{c} E(\mathbf{C}|\mathbf{R} \in \{\mathbf{R}\}_i) f_i \tag{13}$$

where $E(\mathbf{C}|\mathbf{R} \in \{\mathbf{R}\}_i)$ is the best estimate of $\mathbf{C}$ given that $\mathbf{R}$ belongs to class i, and f_i is the probability that $\mathbf{R}$ belongs to class i. The sum is over all possible classes.

Although the membership functions, as defined, are not strictly equal to the probability that the observation $\mathbf{R}_{rs}$ belongs to the particular class, they do represent this probability in a relative sense (i.e., relative to all membership functions for the same pixel). Thus, by normalizing the membership values by the sum of plausible membership values for each pixel, the weights correspond to the probabilities in (13). The retrievals from the different algorithms are the best estimates of the properties given membership to the associated class.

The interpretation of fuzzy membership in terms of mixtures of water types within pixels is not the rationale for this method. However, this interpretation is compelling at times, particularly where we find a blending of retrievals from two adjacent water classes in the image. In a broader sense, the fuzzy logic accommodates ambiguity that exists when differentiating water types based on the remotely sensed information alone. In actuality, class memberships might be exclusive, i.e., pixels might actually belong to only one class, but the information available is incomplete, and thus class assignments are uncertain.

C. Assumptions and Requirements

The effectiveness of our classification method relies on several important assumptions or requirements. First, the clustering process must be able to identify and characterize the classes that exist within the $\mathbf{R}_{rs}$ data. To a large extent, the performance of the class-specific algorithms depends on the effectiveness of the clustering procedure. If there are too few clusters, the clusters will be heterogeneous and the algorithm performance will be compromised. On the other hand, if there are too many clusters, the sample size of stations used to parameterize algorithms will be reduced. Additionally, too many classes can increase the computation time of retrievals, and thus is inefficient. The most important consideration is whether the classes represent physically meaningful differences in the composition of the water. To the extent that this is true, it is worthwhile acquiring a sufficient data base to parameterize algorithms for each class.

One of the biggest problems confronted when using clustering algorithms is identifying the number of correct classes that exist within a given data set [12], [39]. This is generally known as cluster validity, and although a number of cluster validity functions now exist for the FCM method [20], [21], [40], there is no known validity test that is totally reliable. In other words, there is no guarantee from cluster validity functions that the structure imposed by the clustering algorithm is the correct solution. The best job that can be expected from validity functions is to eliminate bad solutions (Bezdek, pers. comm.). In this analysis, we employed two commonly used validity functions, namely, the partition coefficient, F [19], [20], and the compactness and separation index, S [21].

The FCM algorithm requires two key input parameters: the number of classes c and the weighting exponent m. Ideally, the optimal cluster partitioning should arise from the combination of c and m that yields the highest F and the lowest S. As can be seen from Table II, both F and S were sensitive to m, an issue discussed in more depth by Pal and Bezdek [39]. The value of F systematically decreased with increasing m, regardless of c, indicating that as m increased, clusters had greater overlap (a value of 1 signifies no overlap). There was also a tendency for S to decrease as F decreased, although trends in S were not as systematic. Decreasing S indicates that clusters are more compact and separate. It seems somewhat inconsistent for clusters to exhibit greater overlap, while at the same time becoming more compact (smaller S). However, we interpret the validity measures (specifically in regard to F) as indicating inadequate cluster partitions for the higher m values (>2), and hence bad solutions. The lower m values created clusters with less overlap with the least amount at $m = 1.2$ (There are reasons to avoid using m values closer to 1, as explained in Pal and Bezdek, [39]). A c value of 6 performed best according to the F and S measure at $m = 1.2$ and $m = 1.5$. The consistency of $c = 6$ being optimal with these m values is a strong indicator that this is the correct number of clusters. Statistically, the differences between the cluster means and variances at $m = 1.2$ and $m = 1.5$ were insignificant, and we chose $c = 6$ and $m = 1.2$ as being the optimal set of parameters for our data set and the FCM algorithm.

Once the clustering is completed, the statistics generated from the clustering procedure are used to compute the class membership function. The class membership function is based on the proximity of a pixel's $\mathbf{R}_{rs}$ vector to the class mean vector as determined by the squared Mahalanobis distance [equation (11)]. This distance is similar to the Euclidean distance but is scaled with respect to the class covariance matrix. The class mean and covariance matrix are the statistical elements that our model is dependent upon, and therefore it is important that these statistics are representative of the natural classes. Their accuracy depends to a large degree on the class sample sizes, which are used to parameterize or "train" the classification model. The classification loses accuracy when the training sample is too small [41].

A training set is considered small when the number of samples approaches the number of bands n (in this case, $n = 6$). The number of samples (stations) per class ranged from 6 to 65. As a result of this partitioning, some classes were based on small training sets. Small data sets can lead to a covariance matrix that is very different from the true population covariance matrix. Thus, we used a common covariance matrix—the weighted average of all sample covariance matrices, which has been shown to yield higher classification accuracy [42]. Using the common covariance matrix then assumes that the features covary identically for all classes, which may not be the case. However, Hoffbeck and Landgrebe [43] state that even if the covariance matrix of each class is highly different, which is probably not the case here, use of a common covariance

still leads to higher classification accuracy when the training sample sizes are small.

Another requirement is that the *in situ* optical data base contain an adequate representation of water types that naturally exist in the image area. A large amount of time and effort is required to collect bio-optical data. In land remote sensing, it is much easier to differentiate classes since boundaries are generally crisp and spectral differences greater. Furthermore, since land features tend to be more stationary compared to ocean features, classes can be verified with ground-truth data at selected locations. In the ocean, the physical environment is neither stationary nor easily accessible for verification. When optical classes are not known *a priori*, the problem of class identification is not trivial. However, an analysis such as this shows where classes and data exist and where missing classes might be found. The membership maps (Fig. 5) show the presence of classes, and the membership sum map (Fig. 6) shows, among other things, the absence of classes. This information could be used to guide future data collection campaigns.

D. Retrievals

The retrieval images show smooth transitions between water types, even though different algorithms were used in the inversion process. The weighting scheme blends these different algorithms together effectively. However, the optimization scheme (and other optimization algorithms such as the Levenberg–Marquardt method) is susceptible to returning a sub-optimum set of retrieval variables based on a local minimum rather than the global minimum. Such methods also can return physically unrealistic answers. Initial values thus play a crucial role in the outcome of the model. The ambiguity in the possible solutions for the model optimization was minimized by using the OC4 chlorophyll value, which is the standard algorithm applied to SeaWiFS data, and class averages were given as initial values of $b_{bp}(550)$ and $a_g(375)$. By using this set of initial values, the iteration process begins with values that should lie in the vicinity of the global minimum, and the optimization is restricted from converging on physically meaningless retrieval values. Although the final retrieval results were qualitatively acceptable, clearly a rigorous validation program would be required before the algorithms are accepted.

The use of different models, each with its own set of parameters, is aimed at reducing errors introduced by generalized models which fail to capture the natural variation that exists in the ocean environment. It has been shown, for instance, that inversions are sensitive to the parameterization of CDOM absorption [14]. In particular, the exponential slope parameter in a_g models has at least a two-fold variation, with a typical range from 0.011 to 0.019 nm^{-1} [26], [27]). An average value of 0.0145 nm^{-1} is commonly used [22], [28]. The sensitivity analysis of Garver and Siegel [14] demonstrated that retrievals are particularly sensitive to the choice of this parameter. It is therefore important to use a value that is most representative of the water type. Likewise, other parameters influence the overall accuracy of retrievals, and also vary for different water types.

The fuzzy model and weighting scheme are independent of the construction of the semi-analytic models and are not concerned with how the inversion algorithms are implemented. In fact, the scheme does not depend on the use of semi-analytic algorithms; empirical or neural network algorithms could have been used instead. As long as the constituent retrievals are of the same currency (e.g., chlorophyll is retrieved by all algorithms), the fuzzy model can combine their output in a systematic way using the weighting scheme.

One shortcoming is the lack of validation data to test results of the fuzzy classification and weighting of retrievals. At present, limited data sets exist with the full suite of measurements required to develop and parameterize semi-analytic models. Without proper validation data, there is no way to quantitatively validate our image retrievals. However, more emphasis is now being placed on the need for more comprehensive data sets for bio-optical algorithms. The results presented here for one SeaWiFS scene are intended to demonstrate the technique. The coherence of the membership maps and their spatial distribution relative to the *in situ* data suggest that the method is working well in a complex environment such as the northwest Atlantic, where several different water types exist. Although the results are promising, this is only a demonstration of the fuzzy method with ocean color algorithms. More *in situ* data are needed to identify water classes and to characterize their statistical properties. Recent advances in high-quality optical instruments have led to increased availability of optical property measurements in various regions of the oceans. Not only will this lead to a larger data pool to use for water-type classification, it will also yield better algorithms.

V. Summary

Fuzzy classification of ocean color satellite images has been demonstrated. Based on statistics derived by clustering *in situ* reflectance measurements, satellite reflectance measurements have been assigned partial memberships to distinct optical classes. The class memberships were used to derive weighting factors for blending the retrievals from class-specific bio-optical algorithms. This method allows for the existence of a library of algorithms parameterized for different water types, and provides a method for selecting and blending retrievals in a way that avoids the patchwork quilt effect associated with nonweighted or hard-partitioned classification schemes. The initial choice of the number of clusters to be extracted from the *in situ* optical data is crucial. By using two validity functions to evaluate the results of a fuzzy c-means classification, we identified six optically distinct classes in the data set for our region (Table I). The number of classes present will vary from region to region and will depend on the data used. In the future, we believe that a large globally distributed data base can be classified using similar techniques to identify water types. The algorithms parameterized for each water type may be used, regardless of where that type was located in the original *in situ* data base. Like any other remote sensing technique, this method will require validation based on concurrently measured *in situ* and remote sensing measurements.

Acknowledgment

The authors wish to thank A. Barnard, Oregon State University, Corvallis, H. Sosik, Woods Hole Oceanographic Institute,

Woods Hole, MA, C. Roesler, Bigelow Laboratory for Ocean Sciences, West Boothbay Harbor, ME, A. Subramaniam, NOAA Coastal Services Center, Charleston, SC, and M. Kishino, Hokkaido Fisheries Experimental Staion, Hokkaido, Japan, for providing the *in situ* data sets used in this study. They would also like to thank D. Siegel and N. Nelson for their contributions of the Bermuda BBOP data, which we obtained from the SeaBASS archive at NASA GSFC.

REFERENCES

[1] A. Morel and L. Prieur, "Analysis of variations in ocean color," *Limnol. Oceanogr.*, vol. 22, pp. 709–722, 1977.

[2] K. L. Carder, F. R. Chen, Z. Lee, S. K. Hawes, and D. Kamykowski, "Semianalytic moderate resolution imaging spectrometer algorithms for chlorophyll a and absorption with bio-optical domains based on nitrate-depletion temperatures," *J. Geophys. Res.*, vol. 104, pp. 5403–5421, 1999.

[3] O. Frette, J. J. Stamnes, and K. Stamnes, "Optical remote sensing of marine constituents in coastal waters: a feasibility study," *Appl. Opt.*, vol. 37, pp. 8318–8326, 1998.

[4] R. Doerffer and J. Fischer, "Concentration of chlorophyll, suspended matter, and gelbstoff in case II waters derived from satellite coastal zone color scanner data with inverse modeling methods," *J. Geophys. Res.*, vol. 99, pp. 7457–7466, 1994.

[5] R. P. Bukata, J. E. Bruton, and J. H. Jerome, "Application of direct measurements of optical parameters to the estimation of lake water quality indicators," *Environ. Can. Inland Waters Directorate*, vol. 140, no. 35, 1985.

[6] V. I. Burenkov, O. V. Kopelevich, S. V. Sheberstov, S. V. Ershova, and M. A. Evdoshenko, "Bio-optical characteristics of the Aegean Sea retrieved from satellite ocean color data," in *The Eastern Mediterranean as a Laboratory Basin for the Assessment of Contrasting Ecosystems*, P. Malanotte-Rizzoli and V. N. Eremeev, Eds. Noordwijk, The Netherlands: Kluwer, vol. 1999, pp. 313–326.

[7] E. A. Gallie and P. A. Murtha, "Specific absorption and backscattering spectra for suspended minerals and chlorophyll-a in Chilko Lake, British Columbia," *Remote Sens. Environ.*, vol. 39, pp. 103–118, 1992.

[8] F. Wang, "Fuzzy supervised classification of remote sensing images," *IEEE Trans. Geosci. Remote Sensing*, pp. 194–201, Mar. 1990.

[9] J. T. Kent and V. Mardia, "Spatial classification using fuzzy membership models," *IEEE Trans. Pattern Anal. Machine Intell.*, vol. 10, pp. 659–670, Sept. 1988.

[10] J. J. Simpson and R. H. Keller, "An improved fuzzy logic segmentation of sea ice, clouds, and ocean in remotely sensed arctic imagery," *Remote Sens. Environ.*, vol. 54, pp. 290–312, 1995.

[11] L. Zadeh, "Fuzzy sets," *Inform. Contr.*, vol. 8, pp. 338–353, 1965.

[12] A. M. Bensaid, L. O. Hall, J. C. Bezdek, L. P. Clarke, M. L. Silbiger, J. A. Arrington, and R. F. Murtagh, "Validity-guided (re)clustering with applications to image segmentation," *IEEE Trans. Fuzzy Syst.*, vol. 4, pp. 112–123, 1996.

[13] J. E. O'Reilly, S. Maritorena, B. G. Mitchell, D. A. Siegel, K. L. Carder, S. A. Garver, M. Kahru, and C. McClain, "Ocean color chlorophyll algorithms for SeaWiFS," *J. Geophys. Res.*, vol. 103, pp. 24 937–24 953, 1998.

[14] S. A. Garver and D. A. Siegel, "Inherent optical property inversion of ocean color spectra and its biogeochemical interpretation. 1. Time series from the Sargasso Sea," *J. Geophys. Res.*, vol. 102, pp. 18607–18 625, 1997.

[15] J. T. O. Kirk, *Light and Photosynthesis in Aquatic Ecosystems*. New York: Cambridge Univ. Press, 1995, p. 509.

[16] M. Kishino, M. Takahashi, N. Okami, and S. Ishimura, "Estimation of the spectral absorption coefficients of phytoplankton in the sea," *Bull. Marine Sci.*, vol. 37, pp. 634–642, 1985.

[17] A. Morel, K. J. Voss, and B. Gentili, "Bidirectional reflectance of oceanic waters: a comparison of modeled and measured upward radiance fields," *J. Geophys. Res.*, vol. 100, pp. 13 143–13 150, 1996.

[18] H. R. Gordon and D. K. Clark, "Remote sensing optical properties of a stratified ocean: An improved interpretation," *Appl. Opt.*, vol. 19, pp. 3428–3430, 1980.

[19] J. C. Bezdek, *Pattern Recognition with Fuzzy Objective Function Algorithms*. New York: Plenum, 1981.

[20] M. P. Windham, "Cluster validity for the fuzzy c-means clustering algorithm," *IEEE Trans. Pattern Anal. Machine Intell.*, vol. PAMI-4, pp. 357–363, 1982.

[21] X. L. Xie and G. Beni, "A validity measure for fuzzy clustering," *IEEE Trans. Pattern Anal. Mach. Intel.*, vol. PAMI-13, pp. 841–847, 1991.

[22] H. R. Gordon, O. B. Brown, R. H. Evans, J. W. Brown, R. C. Smith, K. S. Baker, and D. K. Clark, "A semianalytical radiance model of ocean color," *J. Geophys. Res.*, vol. 93, pp. 10 909–10 924, 1988.

[23] R. M. Pope and E. S. Fry, "Absorption spectrum (380–700 nm) of pure water, II, Integrating cavity measurements," *Appl. Opt.*, vol. 36, pp. 8710–8723, 1997.

[24] A. C. Rencher, *Methods of Multivariate Analysis*. New York: Wiley, 1995, p. 627.

[25] J. J. O'Reilly *et al.*, "Ocean color chlorophyll a algorithms for SeaWiFS, OC2 and OC4: Version 4," in SeaWiFS Post-Launch Calibration and Validation Analyses. Washington, DC: NASA, vol. 11, ch. 2, to be published.

[26] A. Bricaud, A. Morel, and L. Prieur, "Absorption by dissolved organic matter of the sea (yellow substance) in the UV and visible domains," *Limnol. Oceanogr.*, vol. 26, pp. 43–53, 1981.

[27] K. L. Carder, R. G. Steward, G. R. Harvey, and P. B. Ortner, "Marine humic and fulvic acids: Their effects on remote sensing of ocean chlorophyll," *Limnol. Oceanogr.*, vol. 34, pp. 68–81, 1989.

[28] F. E. Hoge and P. E. Lyon, "Satellite retrieval of inherent optical properties by linear matrix inversion of oceanic radiance models: An analysis of model and radiance measurement errors," *J. Geophys. Res.*, vol. 101, pp. 16 631–16 648, 1996.

[29] A. Morel and Y.-H. Ahn, "Optics of heterotrophic nanoflagellates and ciliates: A tentative assessment of their scattering role in oceanic waters compared to those of bacterial and algal cells," *J. Marine Res.*, vol. 49, pp. 177–202, 1991.

[30] N. G. Jerlov, "Optical studies of ocean water," *Rep. Swedish Deep-Sea Exped.*, vol. 3, pp. 1–59, 1951.

[31] ——, *Marine Optics*. Amsterdam, The Netherlands: Elsevier, 1976.

[32] V. N. Pelevin and V. A. Rutkovskaya, "On the optical classification of ocean waters from the spectral attenuation of solar radiation," *Oceanology*, vol. 18, pp. 278–282, 1977.

[33] L. Prieur and S. Sathyendrenath, "An optical classification of coastal and oceanic waters based on the specific spectral absorption curves of phytoplankton pigments, disolved organic matter, and other particulate materials," *Limnol. Oceanogr.*, vol. 26, 1981.

[34] R. C. Smith and K. S. Baker, "Optical classification of natural waters," *Limnol. Oceanogr.*, vol. 23, pp. 260–267, 1978.

[35] J. T. O. Kirk, "Spectral absorption properties of natural waters: Contribution of the soluble and particulate fractions to light absorption in natural waters," *Aust. J. Marine Freshwater Res.*, vol. 31, pp. 287–296, 1980.

[36] J. M. Mustard and C. M. Pieters, "Photometric phase functions of common geologic minerals and applications to quantitative analysis of mineral mixture reflectance spectra," *J. Geophys. Res.*, vol. 94, no. B10, pp. 13619–13 634, 1989.

[37] P. E. Johnson, M. O. Smith, S. Taylor-George, and J. B. Adams, "A semi-empirical method for analysis of the reflectance spectra of binary mineral mixtures," *J. Geophys. Res.*, vol. 88, no. B4, pp. 3557–3561, 1983.

[38] P. E. Johnson, M. O. Smith, and J. B. Adams, "Simple algorithms for remote determination of mineral abundances and particle sizes from reflectance spectra," *J. Geophys. Res.*, vol. 97, no. E2, pp. 2649–2657, 1992.

[39] N. R. Pal and J. C. Bezdek, "Measuring fuzzy uncertainty," *IEEE Trans. Fuzzy Syst.*, vol. 2, pp. 107–118, 1994.

[40] J. C. Bezdek, W. Q. Li, Y. Attikiouzel, and M. P. Windham, "A geometric approach to cluster validity for normal mixtures," *Soft Comput.*, vol. 1, pp. 166–179, 1997.

[41] T. W. Anderson, *An Introduction to Multivariate Statistical Analysis*, 2nd ed. New York: Wiley, 1984, p. 201.

[42] J. H. Friedman, "Regularized discriminant analysis," *J. Amer. Statist. Assoc.*, vol. 84, pp. 165–175, 1989.

[43] J. P. Hoffbeck and D. A. Landgrebe, "Covariance matrix estimation and classification with limited training data," *IEEE Trans. Pattern Anal. Machine Intel.*, vol. 18, pp. 763–767, July 1996.

Timothy S. Moore received the B.S. degree in electrical engineering from Worcester Polytechnic Institute, Worcester, MA, in 1989, and the M.S. degree in biological oceanography from the Graduate School of Oceanography, University of Rhode Island, Kingston, in 1995. He is currently pursuing the Ph.D. degree at the University of New Hampshire, Durham,

He was an Electrical Engineer with the Naval Undersea Warfare Center, Newport, RI, from 1989 to 1996, programming software for the underwater acoustics department. He became a Research Scientist at the Ocean Process Analysis Laboratory, University of New Hampshire, in 1996, working on bio-optical algorithm development.

Janet W. Campbell was first an Aerospace Technologist with the NASA Langley Research Center, Langley, VA. From 1982 to 1993, she was a Research Scientist at the Bigelow Laboratory for Ocean Sciences. Currently, she is a Research Associate Professor with the Institute for the Study of Earth, Oceans and Space, University of New Hampshire, Durham, where she has taught graduate courses in bio-optical oceanography and ocean remote sensing. She is also a Member of NASA's MODIS and SeaWiFS Science Teams, and has served as Program Manager for Ocean Biology and Biogeochemistry at NASA Headquarters, Washington, DC. She has over 30 years of experience in space technology and ocean remote sensing research. Her research and publications focus on the development of remote sensing techniques utilizing airborne and satellite ocean-color remote sensors to study oceanic primary productivity and biogeochemical processes.

Hui Feng received the B.S. degree in radio physics from East China Normal University (ECNU), Shanghai, China, in 1983, and the M.S. degree in physical oceanography from University of New Hampshire, Durham, in 1996, where he is currently pursuing the Ph.D. degree in oceanography.

From 1983 to 1993, we was a Research Associate with the Institute of Estuarine and Coastal Research, ECNU. His current research interests are in coastal ocean color remote sensing and coastal oceanography.